THE JOURNAL OF BIOLOGICAL CHEMISTRY VOL. 281, NO. 27, pp. 18774–18782, July 7, 2006

Regulation of RhoGEF Activity by Intramolecular and Intermolecular SH3 Domain Interactions*

Received for publication, November 21, 2005, and in revised form, April 24, 2006 Published, JBC Papers in Press, April 27, 2006, DOI 10.1074/jbc.M512482200

Martin R. Schiller[‡§¶1], Kausik Chakrabarti[‡], Glenn F. King[§], Noraisha I. Schiller[‡], Betty A. Eipper[‡§], and Mark W. Maciejewski[§]

From the Departments of [‡]Neuroscience and [§]Molecular, Microbial, and Structural Biology and the [¶]Center for Structural Biology, University of Connecticut Health Center, Farmington, Connecticut 06019-4301

RhoGEFs are central controllers of small G-proteins in cells and are regulated by several mechanisms. There are at least 22 human RhoGEFs that contain SH3 domains, raising the possibility that, like several other enzymes, SH3 domains control the enzymatic activity of guanine nucleotide exchange factor (GEF) domains through intra- and/or intermolecular interactions. The structure of the N-terminal SH3 domain of Kalirin was solved using NMR spectroscopy, and it folds much like other SH3 domains. However, NMR chemical shift mapping experiments showed that this Kalirin SH3 domain is unique, containing novel cooperative binding site(s) for intramolecular P*XX*P ligands. Intramolecular Kalirin SH3 domain/ligand interactions, as well as binding of the Kalirin SH3 domain to the adaptor protein Crk, inhibit the GEF activity of Kalirin. This study establishes a novel molecular mechanism whereby intramolecular and intermolecular Kalirin SH3 domain/ligand interactions modulate GEF activity, a regulatory mechanism that is likely used by other RhoGEF family members.

There are ~69 RhoGEFs in the human genome that are expected to catalyze nucleotide exchange on ~22 Rho GTPases (1). As the major activators of the Rho GTPases, guanine nucleotide exchange factor (GEF)[2] proteins play important roles in cell signaling, rearrangement of the cytoskeleton, membrane trafficking, and translational regulation (2). The widespread effects of GEF domains dictate the need for tight regulation of activity, which is underscored by the observation that deregulation of RhoGEFs is associated with cellular transformation and mental retardation (1, 3).

Most RhoGEFs are composed of tandem Dbl homology (DH) and pleckstrin homology (PH) domains. RhoGEFs are regulated by cellular localization, interaction of phosphoinositides with the PH domain, tyrosine phosphorylation, oligomerization, and other protein/protein interactions (2, 4–8). Although the interaction of phosphoinositides with the PH domain seems to be a general mechanism for modulating GEF activity (5, 6, 9–12), other regulatory mechanisms affect a subset of RhoGEFs. RhoGEFs often contain several domains that are involved in their localization, association with other proteins, and regulation of GEF activity.

Approximately one-third (~22) of the human RhoGEFs contain Src homology 3 (SH3) domains (see Fig. 1). The GEFs with SH3 domains can be grouped into three classes based on the number and arrangement of the domains: Group I, with SH3 domains located N-terminally to the DH and PH domains; Group II, with SH3 domains located C-terminally; and Group III, with multiple SH3 domains. Several pieces of data support the hypothesis that the SH3 domains regulate GEF activity. For example, the cellular transforming activity of Ost is inhibited by its SH3 domain (13), and the first SH3 domain of Trio is necessary for GEF-mediated effects on neurite outgrowth (14).

Regulation of RhoGEFs by SH3 domains could be through an inhibitory intramolecular SH3 domain/ligand association. Most SH3 domains bind to a consensus core Pro-*X*-*X*-Pro (P*XX*P) sequence, with higher affinity derived from additional specificity determinants (15, 16). Intramolecular SH3 domain/P*XX*P interactions regulate several proteins, including Src, Hck, c-Abl, and Tec family tyrosine kinases (8, 17–26). Mixed-lineage kinases are Ser/Thr kinases regulated by an intramolecular SH3 domain interaction (26). $p46^{phox}$ heterodimerizes with and activates NADPH oxidase after an intramolecular SH3 domain/ligand interaction is disrupted (27, 28). $p47^{phox}$ also utilizes intramolecular interactions between its SH3 domains and adjoining linker regions that are autoinhibitory (29). Similarly, an intramolecular interaction between the SH3 and guanylate kinase domains of PSD-95 is disrupted when its SH3 domain binds to a P*XX*P sequence in the protein-tyrosine kinase Pyk2 (30, 31). Clearly, intramolecular SH3 domain/ligand interactions play in important role in the regulation of many proteins, but this has not yet been observed in RhoGEFs.

Eight of the 22 RhoGEFs containing SH3 domains (αPIX, GEF6, βPIX, Q8IVY3, Q9Y2L3, intersectin-1, Trio, and Kalirin) (Fig. 1) also contain at least one consensus P*XX*P SH3 domain ligand-binding sequence between their GEF and SH3 domains. GEFs with SH3 domains preceding or following the DH-PH domains may be regulated by intramolecular SH3 domain/P*XX*P interactions.

In this study, we examined the ability of intramolecular SH3 domain/P*XX*P interactions to contribute to the regulation of GEF activity. We solved the solution structure of the N-terminal SH3 domain of rat Kalirin and found that it contains novel binding site(s) for intramolecular P*XX*P sequences. Interaction of this SH3 domain with internal P*XX*P motifs induces an additional intramolecular association with its neighboring GEF domain, resulting in inhibition of GEF activity. An intermolecular interaction of the P*XX*P motif and SH3 domain with the SH3 domain of the adaptor protein Crk robustly inhibits GEF activity. Thus, the SH3 domain of Kalirin regulates GEF activity through both intra- and intermolecular SH3 domain interactions.

* This work was supported by National Institutes of Health Grants MH65567 and DK32948 and by a University of Connecticut Health Center faculty development award (to M. R. S.). The costs of publication of this article were defrayed in part by the payment of page charges. This article must therefore be hereby marked "*advertisement*" in accordance with 18 U.S.C. Section 1734 solely to indicate this fact.

The atomic coordinates and structure factors (code 1U3O) have been deposited in the Protein Data Bank, Research Collaboratory for Structural Bioinformatics, Rutgers University, New Brunswick, NJ (http://www.rcsb.org/).

The chemical shifts have been deposited in the Biological Magnetic Resonance Data Bank under BMRB accession number 6300 (www.bmrb.wisc.edu/).

[1] To whom correspondence should be addressed: Dept. of Neuroscience, University of Connecticut Health Center, 263 Farmington Ave., Farmington, CT 06019-4301. Tel.: 860-679-4610; Fax: 860-679-1726; E-mail: schiller@nso.uchc.edu.

[2] The abbreviations used are: GEF, guanine nucleotide exchange factor; DH, Dbl homology; PH, pleckstrin homology; SH3, Src homology 3; GST, glutathione *S*-transferase; Kal, Kalirin; HSQC, heteronuclear single quantum correlation; mant-GDP, *N*-methylanthraniloyl-GDP; NaTES, sodium 2-{[2-hydroxy-1,1-bis(hydroxymethyl)ethyl]amino}ethanesulfonic acid; r.m.s., root mean square.

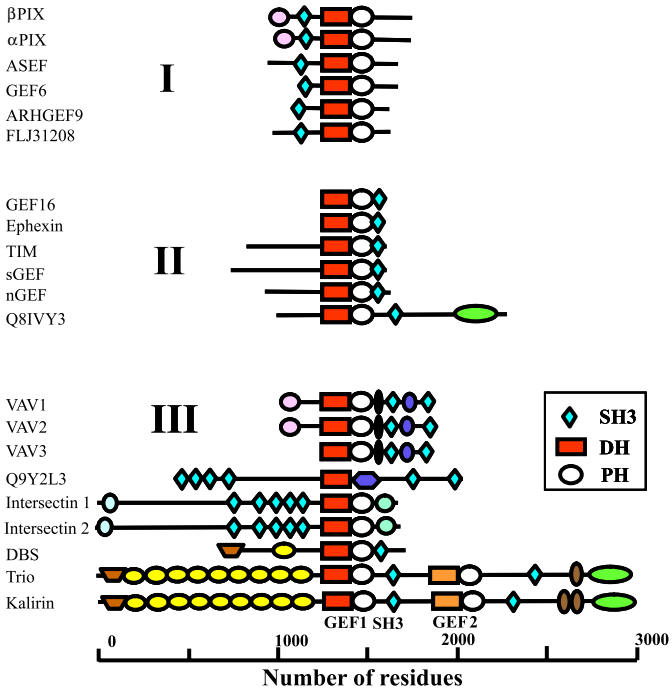

FIGURE 1. **Schematic diagram of human RhoGEFs that contain SH3 domains.** Proteins are grouped according to those that have an SH3 domain N-terminal (Group I) or C-terminal (Group II) to the RhoGEF or that have multiple SH3 domains (Group III). Other domains indicated are the calponin homology (*CH*; *pink circles*), kinase (*green ovals*), protein kinase C conserved region C1 (*black ovals*), SH2 (*blue ovals*), C2 calcium-binding (*turquoise circles*), EPS15 homology (*light blue circles*), Ig/fibronectin type III (*brown ovals*), Sec14p (*brown trapezoids*), and adaptor (*blue hexagon*) domains. *sGEF*, SH3 domain-containing GEF; *nGEF*, neuronal GEF.

EXPERIMENTAL PROCEDURES

SH3 Domain Purification and Structure Determination—^{15}N- and ^{15}N/^{13}C-labeled Kalirin SH3 domains were prepared by overproducing the protein in bacteria as a glutathione *S*-transferase (GST) fusion, purifying the GST fusion protein using glutathione-Sepharose, and recovering the purified labeled SH3 domain proteins in the supernatant after cleavage of the GST-SH3 domain linkage engineered to contain a PreScission protease cleavage site. The resulting protein consists of 12 N-terminal amino acids (GPLGSPGIPGST) from the pGEX-6P vector and Leu^{1637}–Ser^{1706} of the rat Kalirin (Kal) N-terminal SH3 domain (referred to as Kal-SH3). All numbering is according to Kalirin-12a (AF232669) except where indicated. Labeled SH3 domain proteins were dialyzed into 50 mM HEPES (pH 6.4), 150 mM NaCl, and 1 mM dithiothreitol and were supplemented with D_2O to 7.5%. Two- and three-dimensional spectra were recorded on Varian 500- and 600-MHz spectrometers at 25 °C using pulse sequences supplied by the manufacturer. Data were processed using NMRPipe, and peaks were assigned using XEASY (32, 33). The upper bounds for interproton distances were calibrated from the nuclear Overhauser effects using CALIBA (34). Dihedral restraints were based on both TALOS and the $J_{H^NH^\alpha}$ coupling constants determined in a three-dimensional HNHA experiment (35–37).

Chemical Shift Titration Experiments—For chemical shift mapping, titration of PKTP, PLSP, PLPP, AKTP, and tPKTA (where t is trio) peptides (0–8 mM) to ^{15}N-labeled SH3 domain (590–685 μM) was assessed by ^{15}N heteronuclear single quantum correlation (HSQC) analysis. Synthesized peptides were purified by reverse-phase high pressure liquid chromatography, and amino acid sequences were confirmed by Edman degradation and mass spectrometry. The peptide sequences for PKTP, PLSP, and PLPP are shown in Fig. 3. The sequences for AKTP (PIQL**A**KTPAKLRNNSK) and tPKTA (PIHIPKT**A**PAATRQKGR) each have a single Pro-to-Ala substitution in the PKTP sequence (boldface). Peptides were dissolved in the same buffer as the SH3 domain. Chemical shift changes were calculated using the formula $\Delta\delta = (\Delta\delta_H + 0.17\Delta\delta_N)^{1/2}$ (38).

Cell Culture and Transfection—pEAK Rapid cells (an HEK-293 cell variant; Edge BioSystems, Gaithersburg, MD) were maintained in Dulbecco's modified Eagle's medium/nutrient mixture F-12 containing 200 units/ml penicillin G, 20 μg/ml streptomycin sulfate, and 10% fetal bovine serum; plated on polylysine (0.1 mg/ml)-coated dishes; and passaged weekly. Transient transfections were performed using Lipofectamine 2000 and Opti-MEM (Invitrogen) as described by the manufacturer. After a 4-h exposure to the DNA/Lipofectamine 2000 mixture, cells were incubated overnight in Dulbecco's modified Eagle's medium/nutrient mixture F-12 containing 10% fetal calf serum and then for 24 h in serum-free Dulbecco's modified Eagle's medium/nutrient mixture F-12 containing insulin/transferrin/selenium (Invitrogen), penicillin/streptomycin, and 1 mg/ml bovine serum albumin (fatty acid-free) prior to extraction or fixation.

GEF Activity Assays—GEF assays were performed following the release of *N*-methylanthraniloyl-GDP (mant-GDP) from loaded GST-Rac1 or GST-RhoG using purified proteins as described previously (39–41) with modifications. GST-Rac1 expressed in *Escherichia coli* was purified using glutathione-Sepharose as described previously (42) and dialyzed against assay buffer (50 mM HEPES, 100 mM NaCl, and 1 mM dithiothreitol (pH 7.6)) supplemented with 1 mM EDTA and then again with assay buffer lacking EDTA. His/Myc-tagged Kal5, Kal7, Kal8, Kal8(P470A) (PLSA), Kal8(P1573A) (PKTA), Kal8(P1814A) (PLPA), Kal8(P470A/P1573A/P1814A) (ΔP*XX*P), and GEF1 proteins were purified from transfected HEK-293 cells using His·Bind resin (Novagen, Madison, WI) as described by the manufacturer. Before each assay, GST-Rac1 or GST-RhoG (5–20 μM) was loaded with mant-GDP (100 μM) in a volume of 80 μl and supplemented with 10 mM $MgCl_2$. In some experiments, unbound mant-GDP was removed using a NICK™ G-50 column (GE Healthcare). Fluorescence was measured by excitation at 360 nm and emission at 460 nm and was recorded using a Wallac VICTOR^2 Model 1420 96-well plate reader. Reactions were initiated by addition of GTP to 800 μM and 20 μl of Kalirin in reaction buffer. Protein concentrations were determined by bicinchoninic acid assay (Pierce) or by densitometry of Coomassie Blue-stained gels using bovine serum albumin as a standard. In some cases, initial reaction rates (with buffer background rates subtracted) are reported in a bar graph ($n = 3$) with standard deviations. Statistical analysis was performed using a non-parametric one-way analysis of variance with a Newman-Keuls algorithm to determine significant differences or Student's one-tailed *t* test.

Activation of Rac2 in HEK-293 cells transfected with Kalirin plasmids (cotransfected with pEBB-Crk1 in some experiments) was analyzed using a GST effector protein binding assay kit (Upstate Biosystems, Lake Placid, NY) (43). PCR analysis of cDNA from HEK-293 cells showed the presence of Rac2, but not Rac1. For Rac activation assays, cell supernatants prepared in MLB buffer (25 mM HEPES, 150 mM sodium chloride, 1% Nonidet P-40, 10 mM magnesium chloride, 1 mM EDTA, 10% glycerol, 0.3 mg/ml phenylmethylsulfonyl fluoride, 1.0 mM sodium vanadate, and protease inhibitors (pH 7.5)) (44) were incubated with glutathione-agarose beads containing immobilized Pak (p21-activated kinase) p21 binding domain (residues 67–150; 10.0 μg), and unbound protein was removed with three washes of MLB buffer.

Far-Western SH3 Domain Array Analysis—Far-Western analysis was performed using extracts prepared from HEK-293 cells transfected with pEAK10-Kal8 and an array containing 38 different GST-SH3

domain proteins (referred to as GST-SH3) spotted at two different concentrations (*version* 1.00; Panomics, Fremont, CA). The array membrane was blocked with phosphate-buffered saline and 5% dehydrated milk for 30 min, washed, and incubated with cell extracts (800 μl) in 6.0 ml of phosphate-buffered saline supplemented with 0.5% Triton X-100 and 0.3 mg/ml phenylmethylsulfonyl fluoride. Arrays were washed three times with Tris-buffered saline/Tween 20 and then analyzed by Western blotting using anti-Myc monoclonal antibody 9E10, which recognizes the Myc tag at the N terminus of transfected Kal8. A control Western blot analysis showed that anti-Myc antibody recognized only the transfected protein (data not shown).

Co-immunoprecipitation—For Kal8-Crk co-immunoprecipitation experiments, HEK-293 cells were cotransfected with expression constructs for Myc-Kal8 or Myc-Kal8(PKTA) and for Crk1 or Crk1(W170K). Cell lysates (10% (w/v)) were prepared in 50 mM HEPES (pH 7.6), 150 mM NaCl, 10% glycerol, and 0.5% Triton X-100 with a mixture of protease inhibitors (44). Insoluble material was removed by centrifugation at 16,000 × *g* for 30 min. Lysate (200 μg) was incubated with antiserum as indicated for 2 h with shaking and then centrifuged at 10,000 × *g* for 10 min to remove any insoluble material. Immune complexes were incubated with protein G-Sepharose (Amersham Biosciences, Uppsala, Sweden) for 1 h and washed three times with buffer. Proteins were eluted by boiling in SDS-PAGE sample buffer and analyzed by Western blotting.

GST Pulldown Assay—GST pulldown experiments were used to analyze GEF1 binding to the SH3 domain, Crk binding to different fragments of Kal7 and Kal8, and Kal5 binding to Crk1. Each GST-Kalirin chimera was purified from *E. coli* BL21 or Rosetta (Novagen) using glutathione-Sepharose or glutathione-agarose as described previously (42). The GST fusion proteins included amino acids 517–976 for spectrin repeats 4–7, Lys^{1274}–Arg^{1575} for GEF1, Lys^{1274}–Met^{1454} for the DH1 domain, Ser^{1453}–Arg^{1575} for the PH1 domain, Thr^{1615}–Val^{1644} for the Kal7 C terminus (AF230644) (45), Ser^{1453}–Ser^{1706} for the PH-linker-SH3 domain, and Leu^{1637}–Ser^{1706} for the SH3 domain. To assess GEF binding to Kal-SH3, the His/Myc-tagged Kalirin GEF1 domain (referred to as Kal-GEF1) was prepared from transfected 293 cells using His•Bind affinity resin as described by the manufacturer. GST-SH3 (5 μg) or this domain preincubated with 0.5 mM PLSP, PKTP, PLPP, or AKTP peptide was incubated with Kal-GEF1 in MLB buffer for 1 h with shaking at 4 °C. Similar experiments were performed using purified Myc-Kal5 instead of Kal-GEF1. The affinity resin was washed three times with 500 μl of cold MLB buffer. To map the Crk-binding site in Kalirin, Crk1 was prepared as described for the GST-Kalirin chimera and incubated with thrombin to release Crk1 from GST; Crk1 protein was recovered from the supernatant. Individual GST-Kalirin fusion proteins (5 μg) were incubated with purified Crk1 (100 ng) in 900 μl of TMT buffer (20 mM NaTES, 10 mM mannitol, and 1% Triton X-100 (pH 7.4)) for 2 h with shaking at 4 °C. Protein complexes isolated with glutathione-Sepharose or glutathione-agarose were washed once with 500 μl of cold TMT buffer. For each experiment, proteins bound to the beads were eluted by boiling in SDS-PAGE sample buffer. Samples were analyzed by Western blot analysis, and blots were also stained with Coomassie Blue R-250.

RESULTS

Kal-SH3 Has a Structure Similar to That of Other SH3 Domains—DH proteins containing SH3 domains are a major subgroup of RhoGEFs. We determined the structure of Kal-SH3 by NMR spectroscopy as a basis for investigating the role of SH3 domains in regulating GEF activity. ^{15}N- and $^{15}N/^{13}C$-labeled SH3 domains were purified (Fig. 2*A*, *arrow*) and used to solve the structure. Sequential assignments were determined from HNCACB and HN(CO)CACB experiments. Assignments of side chain carbons and protons were determined using C(CO)NH and HC(CO)NH total correlated spectroscopy and HCCH COSY experiments. Long- and short-range distance constraints were determined from ^{15}N-edited nuclear Overhauser effect-HSQC and ^{13}C-edited HSQC-nuclear Overhauser effect spectra. Torsion angle restraints (ϕ and ψ) were determined using TALOS, and ϕ angle restraints were validated using an HNHA experiment (37). Restraints for χ_1 angles were determined from an HNHB spectrum. Hydrogen exchange experiments were unsuccessful, so hydrogen bond restraints were included only for internal β sheet residues that showed strong backbone amide proton couplings. Structure calculations were performed using CYANA and further refined using X-PLOR with experimental distance and angle constraints as described (36, 46).

Structural statistics are shown in Fig. 2*B*. The structure has backbone and side chain root mean square (r.m.s.) deviations similar to or better than those of other SH3 domain structures determined by NMR (*e.g.* Protein Data Bank codes 1AON, 1AEY, 1ARK, 1AWW, and 1H3H). Superposition of the backbone for an ensemble of 20 lowest energy structures is shown as a stereo image in Fig. 2*C*. Kal-SH3 has a fold similar to those of other SH3 domains, with three pairs of antiparallel β strands connected by RT-Src, n-Src, and distal loops and a 3_{10} helix (Fig. 2*D*). Alignment of the SH3 domain protein backbone with that of the representative Sem5 C-terminal SH3 domain (Fig. 2*E*) shows similar tertiary folds (r.m.s. deviation of 1.8 Å). A search for proteins with similar three-dimensional structures using DALI identified several SH3 domains, with α-spectrin (Protein Data Bank code 1TUD) and melanoma-derived growth regulatory protein (code 1I1J) producing the lowest r.m.s. deviations (2.0 Å) (47). One of the most notable differences in the Kal-SH3 structure is reorganization of the loops. A *cis*-Pro peptide bond in the distal loop of Kal-SH3 (Fig. 2*D*, *red arrow*) was assigned on the basis of strong nuclear Overhauser effects between H^{α} and NH of Ser^{63} with H^{α} of Pro^{64}. This is the first reported *cis*-Pro in the distal loop of an SH3 domain. The Ser^{63}-Pro^{64} sequence is conserved in Kalirin proteins from human, mouse, rat, frog, pufferfish, and chicken, and we anticipate that the *cis*-Pro peptide bond is also conserved in these paralogs. The SH3 domain of the RhoGEF protein Vav has a *cis*-Pro in its RT-Src loop that regulates intra- and intermolecular SH3 domain interactions (38).

Kal-SH3 Binds to Internal PXXP Motifs, Suggesting an Intramolecular SH3 Domain/Ligand Interaction—Kal8 contains three consensus SH3 domain recognition motifs (P*XX*P) that might interact with SH3 domains: one in spectrin repeat 3 (PLSP), one in the linker between the GEF and SH3 domains (PKTP), and one C-terminal to the SH3 domain (PLPP) (Fig. 3*A*). To test whether the SH3 domain binds any of these P*XX*P motifs, 16-residue peptides encompassing these sequences (Fig. 3*A*) were synthesized. HSQC chemical shift analysis was used to examine whether any of the peptides interact with Kal-SH3. The three peptides bound to the SH3 domain with varying affinities.

An overlay of HSQC spectra for the SH3 domain in the absence and presence of the PKTP peptide (at ~50% saturation) is shown in Fig. 3*B*. The majority of PKTP-induced chemical shift movements were <0.05 ppm ($\Delta^{15}N + 0.17^{13}C$), indicating that the gross conformation of the protein did not change; however, significant reproducible shifts for several backbone amide resonances were observed. Binding of the PKTP peptide was next analyzed by chemical shift titration. The *inset* in Fig. 3*B* shows the change in chemical shift of the His^{30} cross-peak with increasing concentrations of PKTP. A select group of resonances showed similar dose-dependent shifts of >0.15 ppm upon addition of the PKTP peptide (Fig. 3*C*).

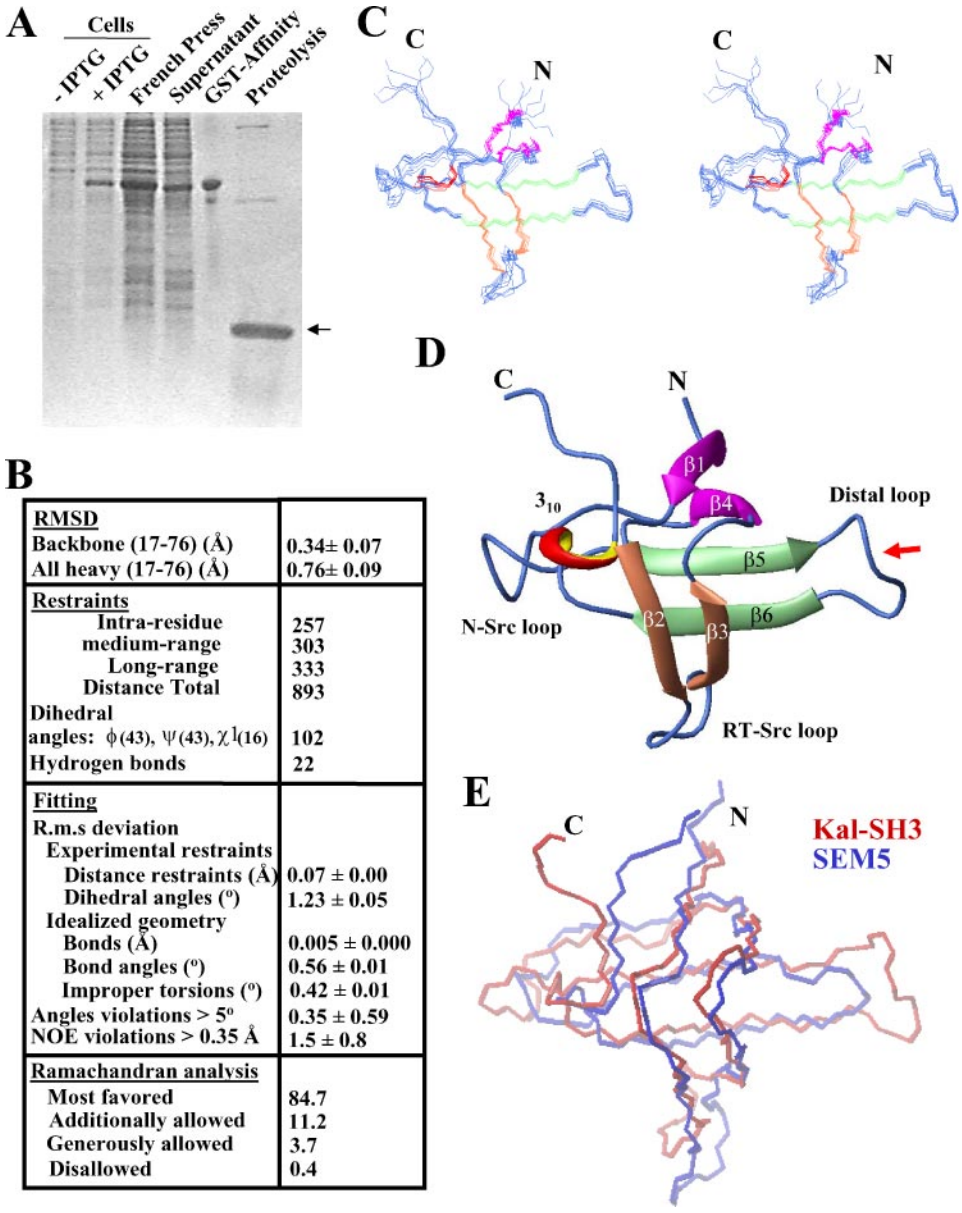

B

RMSD	
Backbone (17-76) (Å)	0.34± 0.07
All heavy (17-76) (Å)	0.76± 0.09
Restraints	
Intra-residue	257
medium-range	303
Long-range	333
Distance Total	893
Dihedral angles: $\phi(43)$, $\Psi(43)$, $\chi 1(16)$	102
Hydrogen bonds	22
Fitting	
R.m.s deviation	
Experimental restraints	
Distance restraints (Å)	0.07 ± 0.00
Dihedral angles (°)	1.23 ± 0.05
Idealized geometry	
Bonds (Å)	0.005 ± 0.000
Bond angles (°)	0.56 ± 0.01
Improper torsions (°)	0.42 ± 0.01
Angles violations > 5°	0.35 ± 0.59
NOE violations > 0.35 Å	1.5 ± 0.8
Ramachandran analysis	
Most favored	84.7
Additionally allowed	11.2
Generously allowed	3.7
Disallowed	0.4

FIGURE 2. **Structure of Kal-SH3.** *A*, Coomassie Blue-stained gel showing various steps in the production and purification of recombinant ^{15}N-labeled SH3 domain. The *arrow* indicates SH3 domain protein used for structural determination. *IPTG*, isopropyl β-D-thiogalactopyranoside. *B*, structural statistics for the calculated ensemble of SH3 domain structures. 20 structures calculated with CYANA were energy-minimized in X-PLOR. r.m.s. deviations (*RMSD*) were calculated against the mean. Ramachandran analysis was performed with PROCHECK Version 3.4.4. All statistics are means ± S.D. *NOE*, nuclear Overhauser effect. *C*, overlay of the ensemble of 20 SH3 domain structures for the best fit of residues 17–76. Loops are colored *blue*, and the N and C termini are indicated. Pairs of antiparallel β sheets are colored *magenta* (β1 and β4), *orange* (β2 and β3), and *pale green* (β5 and β6). *D*, ribbon diagram of the SH3 domain with secondary structural elements, loops, and termini labeled. Color and orientation are the same as described for *C*. The *red arrow* indicates the distal loop where the *cis*-Pro bond is located. *E*, Kal-SH3 backbone (residues 17–78; *red*) fit to backbone residues for the Sem5 SH3 domain (residues 155–211; *blue*; Protein Data Bank code 2SEM) using the program MolMol. The r.m.s. deviation for peptide backbone Kal-SH3 and Sem5 residues in secondary structural elements is 1.8 Å.

A representative chemical shift plot for Glu^{18} illustrated a cooperative binding isotherm that was typical for each residue showing significant chemical shift changes (Fig. 3*D*). All peaks approached saturation near a 1.5-fold molar ratio of the PKTP peptide to the SH3 domain, with an average midpoint value of 410 ± 68 μM (n = 17) upon fitting to a sigmoidal curve. At SH3 domain/PKTP peptide molar ratios of >1, we observed numerous peaks that began to disappear while new peaks began to appear, indicating a conformational change (data not shown). Presumably, after saturation of the first binding site, a second binding event induces a conformational change. The cooperative binding curves observed for the chemical shift titration experiments could be explained by the presence of two PKTP ligand-binding sites or by multimerization of the SH3 domain. Because the peak line widths did not change, we favor two P*XX*P-binding sites. A Hill plot of the titration data for Glu^{18} was similar to those for other residues, yielding a Hill coefficient of 2.5 ± 0.6 (n = 4), supporting cooperative binding and the hypothesis that Kal-SH3 has two binding sites for the PKTP peptide ligand (Fig. 3*E*).

Of the three Kal8 P*XX*P motif peptides tested, the PKTP peptide showed the highest affinity for the SH3 domain (Fig. 3*F*). The PKTP peptide showed cooperative binding curves (Fig. 3*D*), whereas the PLSP peptide (located in spectrin repeat 3) produced a typical non-cooperative binding isotherm. Fitting the data to a standard binding isotherm equation yielded a K_d of 552 ± 104 μM (n = 5) (Fig. 3*F*) (48). At the maximal PLPP peptide (located C-terminal to the N-terminal SH3 domain) concentration of 760 μM, the binding isotherms did not approach saturation, precluding calculation of a Hill coefficient or binding constant. The majority of residues affected by the PLPP and PLSP peptides were also affected by the PKTP peptide; however, PLPP and PLSP binding each affected a largely different subset of these residues. These chemical shift mapping experiments suggest that PLPP and PLSP bind to different sites on the SH3 domain and that PKTP binds to both of these sites.

The intramolecular interaction between the PKTP peptide sequence N-terminal to the SH3 domain and the SH3 domain is of modest affinity (midpoint value of 410 μM). For an intermolecular protein/protein interaction, we must consider whether this affinity is biologically relevant. If we approximate the PKTP ligand concentration in an intramolecular interaction by assuming that the ligand is constrained to a 19-nm

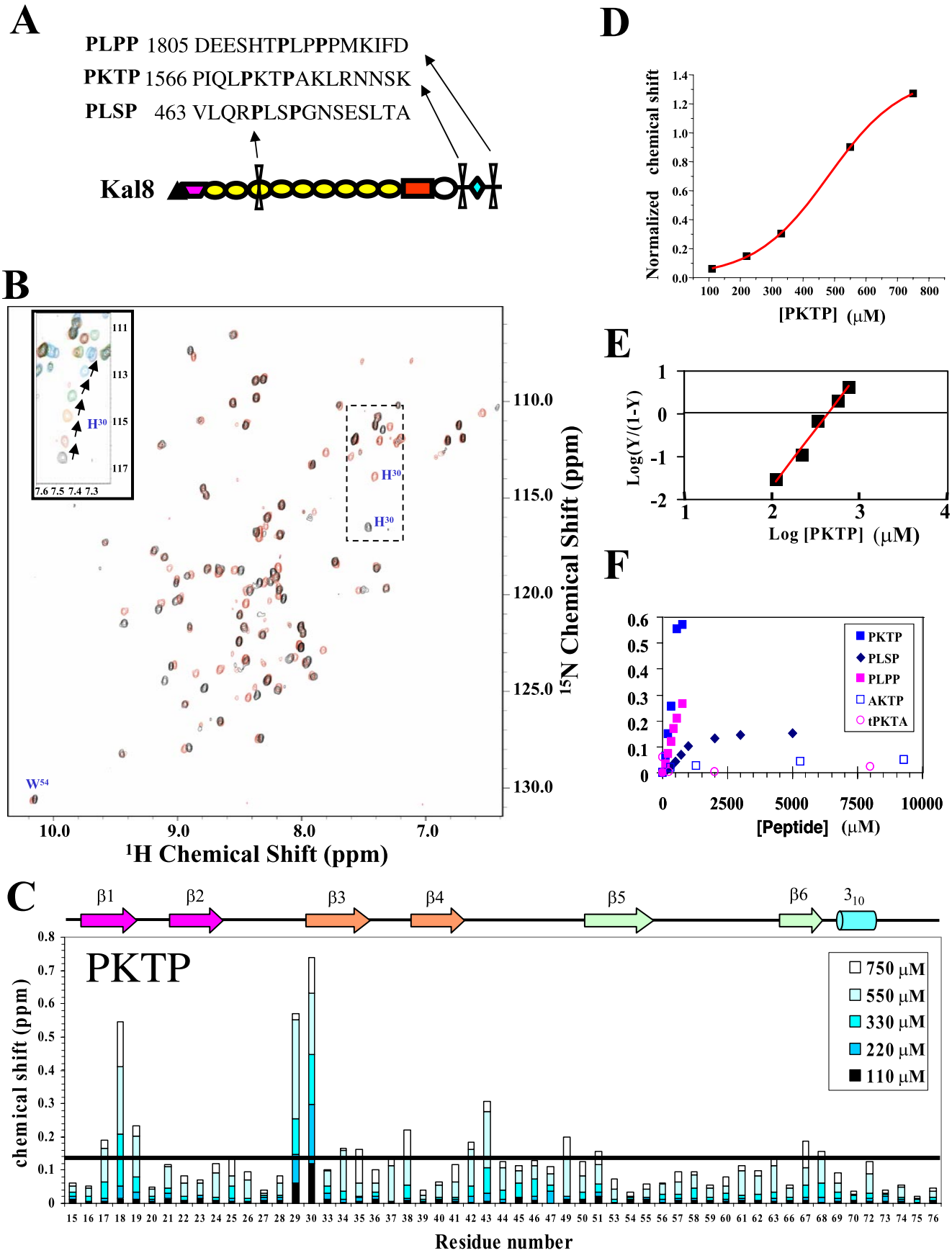

FIGURE 3. **Kal-SH3 binds intramolecular P*XXP* peptides.** *A*, schematic representation of Kal8 with the location and identification of P*XX*P peptides. Domains are as described in the legend to Fig. 1. *B*, overlaid ^{15}N-edited HSQC spectra of labeled SH3 domain without (*black peaks*) and with (*red peaks*) 330 μM PKTP peptide. Trp^{54} side chain and His^{30} backbone amide resonances are labeled. The *inset* is an expanded view of the area bordered by *dashed lines* and shows migration of the His^{30} backbone amide cross-peak with increasing

diameter sphere (based on a linear extension of 47 amino acids between the SH3 domain and the PKTP motif), its effective concentration would be ~20 mM, far greater than the affinity of the SH3 domain for this peptide. Given these relative affinities and concentrations, an intramolecular SH3 domain/PKTP interaction should be highly favored over a homodimeric intermolecular interaction. In this situation, we would expect the Kal-SH3/PKTP interaction to breathe frequently, making both the SH3 domain and its ligand available for interaction with other SH3 domains or SH3 domain ligands. The affinity of this intramolecular SH3 domain-PKTP complex is similar to that reported for the intramolecular interaction between the Tec SH3 domain and its adjoining P*XX*P motif (K_d = 2.0 mM) (23). Even artificially juxtaposing a P*XX*P motif next to an SH3 domain can generate an intramolecular SH3 domain-P*XX*P motif complex (49). Furthermore, weak protein/protein interactions with similar affinities have biological significance (50).

Prolines in the PKTP Peptide Are Required for Its Interaction with Kal-SH3—To test whether the proline residues in the PKTP motif are critical for its interaction with the SH3 domain, we examined whether Kal-SH3 bound PKTP peptides with Pro-to-Ala mutations. The AKTP peptide has the N-terminal proline mutated to alanine, and a peptide corresponding to the same region in Trio has the C-terminal proline substituted with alanine (tPKTA). These peptides induced small chemical shift changes only at high concentrations. At similar concentrations, these peptides yielded chemical shift changes that were substantially less than those of the PKTP peptide (Fig. 3*F*), indicating that each of the two prolines in the PKTP peptide is important for interaction with Kal-SH3.

Kal-SH3 Contains a Novel Binding Site(s) for PXXP Ligands—The cooperative binding isotherms suggest that the PKTP peptide binds to two sites on the SH3 domain. Residues showing peptide-induced chemical shift changes were mapped onto the surface of the SH3 domain (Fig. 4*A*, *PKTP*). A 180° rotation is shown for each surface map to allow viewing of all residues affected by peptide ligands. The PKTP peptide bound to a contiguous stretch of residues on both faces of the protein. Because the PLSP peptide showed a typical exponential binding isotherm, we mapped its binding site. The residues affected defined a subset of residues affected by PKTP, suggesting a single binding site for PLSP (Fig. 4*A*, *PLSP*). The majority of residues affected by PLSP (Ala^{29}, Ser^{30}, Glu^{33}, Leu^{45}, Glu^{46}, Arg^{47}, Ser^{49}, and Arg^{51}) mapped to a cluster of residues in the RT-Src and n-Src loops (Fig. 4*A*, *PLSP*), and nearly all were also affected by the PKTP peptide. These residues define putative binding site 1 (colored *blue*; referred to hereafter as site 1).

Titration with the PKTP peptide also showed shifts in a second cluster of residues (Fig. 4*A*, colored *green*). Titration with the PLPP peptide (Fig. 4*A*, *PLPP*, colored *green*) affected this same cluster of residues (Cys^{17}, Glu^{18}, Leu^{19}, Leu^{34}, Val^{42}, Glu^{43}, Leu^{44}, and Gly^{68}) and three additional residues in the RT-Src loop of site 1 (colored *blue*). This second cluster is hereafter referred to as site 2 and mapped to the β1, β4, and β6 strands.

To compare sites 1 and 2 in Kal-SH3 with the ligand-binding sites of other SH3 domains, the Kal-SH3 sequence was aligned with sequences of other SH3 domains with known structure and ligand-binding sites, and the putative canonical P*XX*P ligand interaction site was mapped onto the surface of Kal-SH3 (Fig. 4*A*, *Canonical*). Surprisingly, both sites 1 and 2 in Kal-SH3 were at a different location than the canonical ligand-binding site observed in most other SH3 domains. Together, the observed cooperative binding curves, a Hill coefficient of >2, and mapping of different binding sites strongly support the presence of two cooperative P*XX*P-binding sites in Kal-SH3. Although unlikely, even if Kal-SH3 has just one P*XX*P motif-binding site, it is distinct from the canonical site in most other SH3 domains and indicates a unique property of Kal-SH3.

To gain further insight into the novel SH3 domain ligand-binding site(s), we compared the sequences of eight Kalirin orthologs and paralogs from several species (Fig. 4*B*, *upper*). Residues in site 1 (colored *blue*) had 43% amino acid identity, whereas residues in site 2 (colored *green*) were 75% conserved among the eight species examined. We compared conservation of these sites in Kalirin with that in eight SH3 domains with identified P*XX*P-binding sites that we randomly selected from the Protein Data Bank (Fig. 4*B*, *middle*, colored *magenta*). Of the 8–17 amino acids involved in binding P*XX*P ligands in the typical SH3 domain proteins, only one completely conserved Trp residue was identified. The level of conservation of the canonical binding site between the Grb2 and Sem5 orthologs is similar to that observed for sites 1 and 2 between Kalirin orthologs and paralogs. These sequence comparisons demonstrate that P*XX*P sites 1 and 2 are conserved in Kalirin homologs. Moreover, the P*XX*P-binding site(s) in Kal-SH3 are distinct from those in other non-canonical SH3 domain ligand-binding sites (Fig. 4*B*, *lower*, colored *magenta*).

Intramolecular SH3 Domain/PXXP Peptide Interactions Control the Catalytic Activity of Kal-GEF1—Intramolecular interactions of SH3 domains with P*XX*P motifs control the activities of tyrosine kinases, mixed-lineage kinases, and several other proteins (8, 17–26). We wanted to determine whether intramolecular Kal-SH3/P*XX*P interactions regulate the exchange activity of the Kalirin N-terminal GEF domain. Kalirin is a RhoGEF for the Rho GTPases Rac1 and RhoG (42, 45). We examined whether the intramolecular SH3 domain/PKTP interaction modulates the activity of Kal-GEF1 toward Rac1 in fluorogenic GEF assays with purified fragments of Kalirin (Fig. 5*A*) (41). The activity of Kal-GEF1 was not significantly affected by addition of either Kal-SH3 or the PKTP peptide alone. However, in the presence of an excess of both Kal-SH3 and the PKTP peptide, GEF activity was reduced by ~4-fold compared with the activity of Kal-GEF1. These results suggest that an intramolecular SH3 domain-PKTP complex can inhibit GEF activity.

We therefore investigated whether the SH3 domain/PKTP interaction with the GEF domain functions similarly within full-length Kal8. Fluorogenic GEF assays with GST-Rac purified from bacteria and full-length Kal8 purified from transfected HEK-293 cells were used to test this model. Kal8 catalyzed nucleotide exchange on 3.8 μM GST-Rac1 with a turnover rate of 5 molecules/h, ~1/20th the rate of GST-Rac1 exchange catalyzed by the isolated Kalirin GEF1 domain (114 molecules/h). This difference demonstrates the presence of potent inhibitory interactions within Kal8 (Fig. 5*B*). The three Kal8 proteins mutated at each individual P*XX*P site were each purified and assessed for GEF activity; the activity of each mutant Kal8 protein was similar to that of wild-type Kal8 (data not shown).

concentrations of PKTP peptide (0 μM (*black*), 110 μM (*red*), 220 μM (*orange*), 330 μM (*green*), 500 μM (*cyan*), and 750 μM (*blue*). *C*, titration plot showing the distance each SH3 domain backbone amide resonance moves as the concentration of PKTP peptide is increased. Colors correspond to the concentration of peptide as indicated. Cys^{17}, Glu^{18}, Leu^{19}, Ala^{29}, His^{30}, Glu^{33}, Leu^{34}, Val^{42}, Glu^{43}, Leu^{45}, Ser^{49}, Arg^{51}, Glu^{67}, and Gly^{68} show chemical shift changes of >0.15 ppm (*black line*). *D*, binding isotherm for the PKTP peptide and SH3 domain showing the dose dependence of changes in Glu^{18} chemical shifts. Data were fit to an equation for a sigmoidal curve (*red*). Normalized changes in chemical shifts are derived from the following equation: $(\delta_{obs} - \delta_{initial})[PXXP]/(\delta_{final} - \delta_{initial})[SH3]$. *E*, Hill plot for binding of the PKTP peptide to the SH3 domain based on the chemical shifts of Glu^{18}. *F*, chemical shift titration for the response of Ala^{29} to the PKTP, PLSP, PLPP, AKTP, and tPKTA peptides. In *B–F*, [SH3 domain] = 590 μM, except for the titration of the PLPP peptide in *F*, where [SH3 domain] = 685 μM. For quantitation of all chemical shifts, the ^{15}N dimension is scaled by a factor of 0.17 relative to the ^{1}H dimension (38).

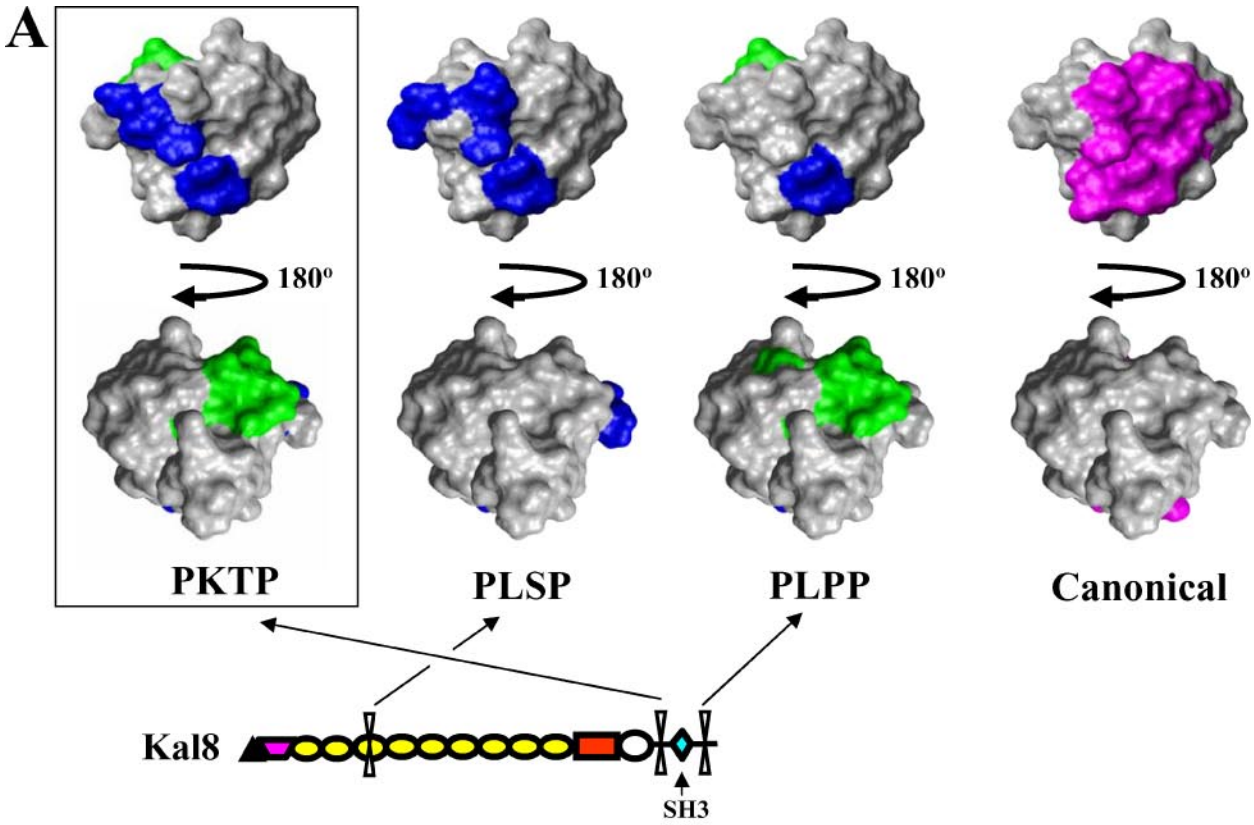

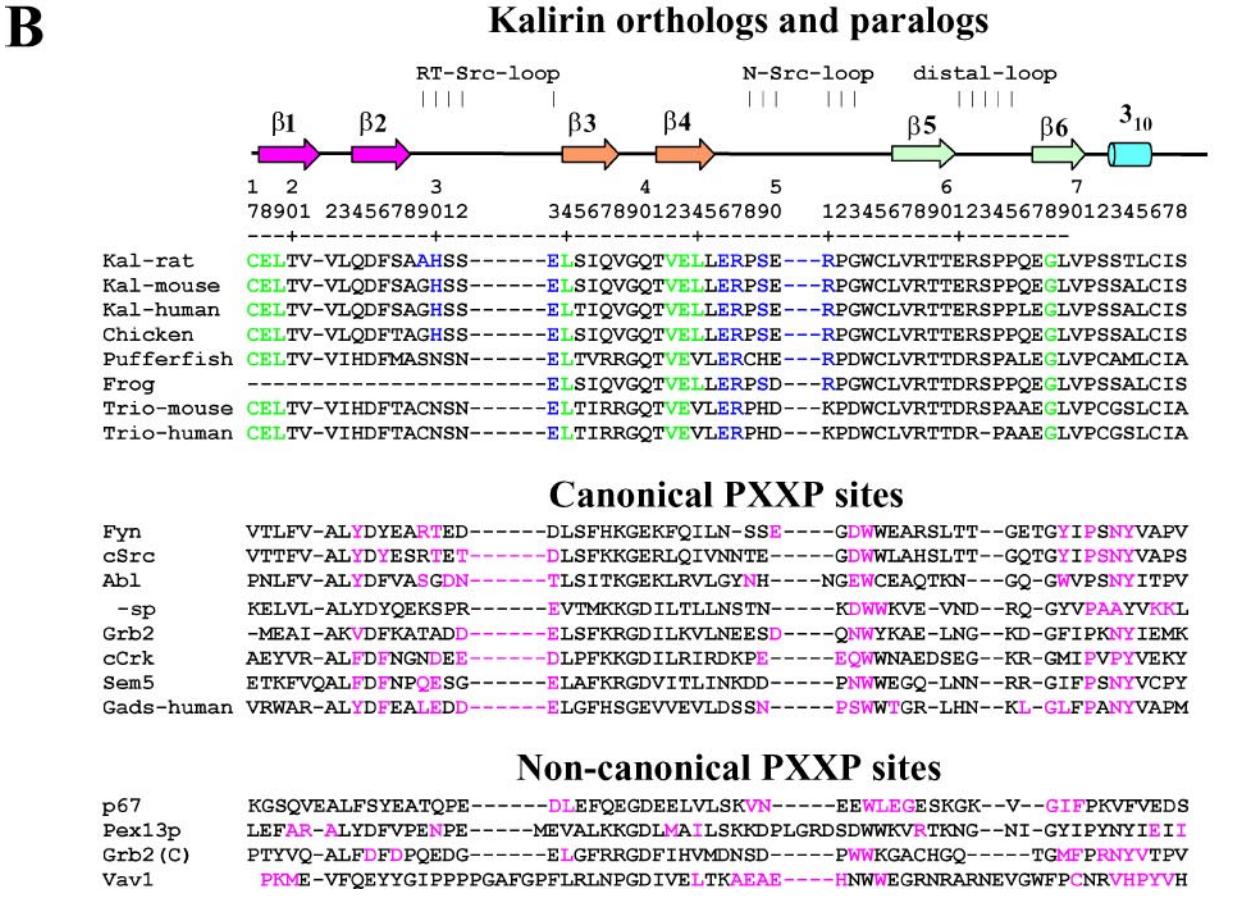

FIGURE 4. **Mapping of two potential sites on Kal-SH3 for binding of intramolecular P*XXP* motifs.** *A*, molecular surface representations of Kal-SH3 showing residues affected upon interaction with various P*XX*P peptides. The *lower* surface plots represent an 180° rotation about the *z* axis of the *upper* surface plots. Residues showing chemical shifts upon interaction with the P*XXP* peptide are colored as follows. Background was defined as the maximal chemical shift observed for residues in the N and C termini, which are disordered

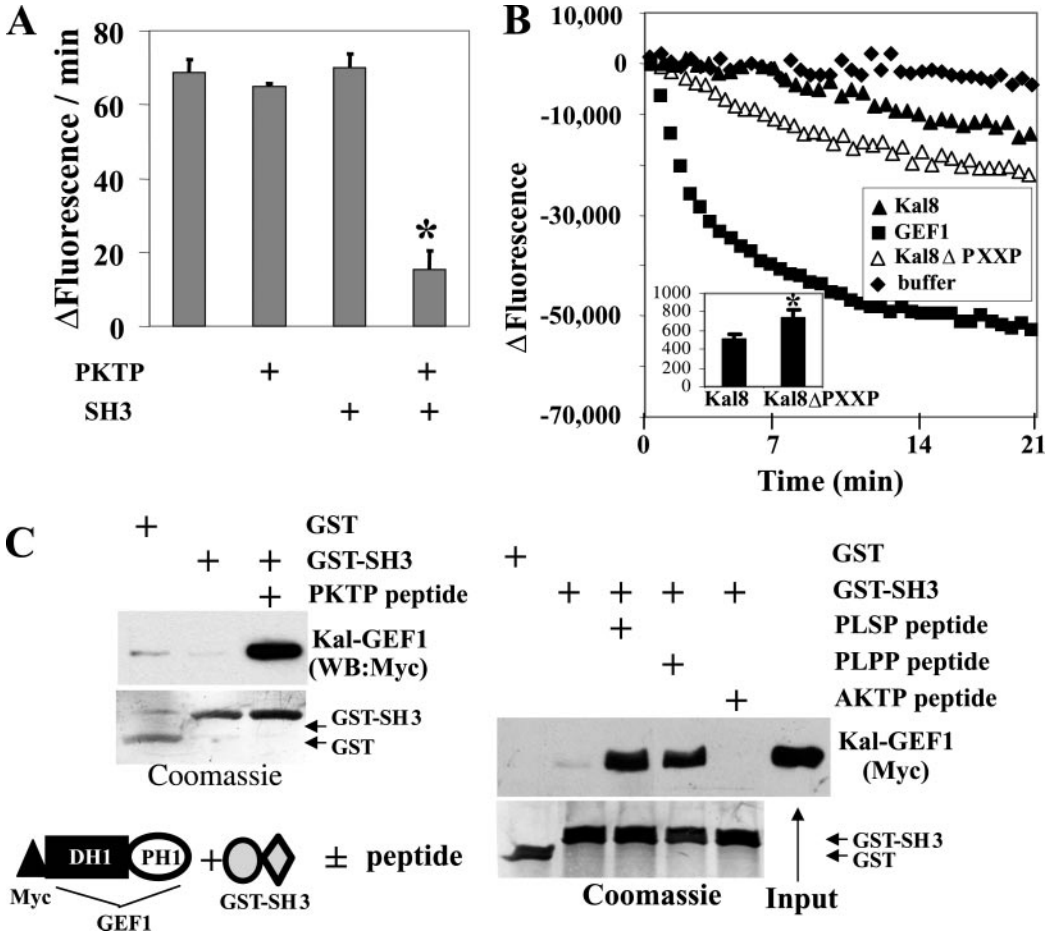

FIGURE 5. **An intramolecular SH3 domain/ligand interaction regulates an interaction between the SH3 and GEF domains of Kal8.** *A*, *in vitro* GEF assay following release of fluorescent mant-GDP from loaded GST-Rac1 (19 μM). Reactions (100 μl) contained Kal-GEF1 purified from transfected 293 cells (1.1 μM), the PKTP peptide (0.5 mM), and GST-Kal-SH3 (655 μM) as indicated. The background rate of mant-GDP release was subtracted from reported values. *Error bars* represent S.D. values ($n = 3$). *, significant difference from control ($p < 0.001$). *B*, representative *in vitro* GEF assays using GST-Rac1/mant-GDP (3.8 μM) as a substrate for GST-GEF1, Kal8, or Kal8ΔP*XXP* (3.1 nM). The *inset* shows the rate of fluorescence change/min for Kal8 and Kal8ΔP*XXP* ($n = 6$; $p < 0.0001$) *C*, Myc-tagged Kal-GEF1 purified from transfected 293 cells (9 μM) and incubated with GST or GST-SH3 with or without various peptides (0.5 mM) as indicated. The amount of Myc-tagged Kal-GEF1 bound was assessed by a pulldown assay using glutathione-Sepharose, followed by Western blot (*WB*) analysis with anti-Myc antibody.

Because all three P*XX*P motifs in Kal8 bound to Kal-SH3, we generated a Kal8 protein mutated at all three sites (Kal8ΔP*XX*P). When purified and assayed using Rac1, Kal8ΔP*XX*P was 1.5 ± 0.1-fold more active than wild-type Kal8 or Kal8 with a single P*XX*P motif mutated (Fig. 5*B*, *inset*). Similar results were obtained using GST-RhoG as a substrate (data not shown). Although intramolecular SH3 domain/ligand regulation of GEF activity was less pronounced in wild-type Kal8 (Fig. 5*B*) than in isolated fragments (Fig. 5*A*), both experiments provide evidence that P*XX*P motifs in Kalirin bind to its SH3 domain and inhibit GEF activity. The differences in these experiments (1.5-fold *versus* 4-fold) may be due to steric restriction of the domains involved. In addition to the modest role of the intramolecular SH3 domain/P*XX*P interaction in modulating the GEF activity of Kal8, more potent regulatory mechanisms remain to be identified.

Kal-SH3/PXXP Ligand Interactions Facilitate Association with the GEF Domain—The effect of intramolecular SH3 domain/P*XX*P interactions on GEF activity suggests that the SH3 domain-P*XX*P complex binds to the GTPase or directly to the GEF1 domain. To test whether Kal-SH3 binds to Kal-GEF1, we performed GST pulldown experiments. Myc-tagged Kal-GEF1 purified from transfected HEK-293 cells was incubated with GST or GST-SH3 in the absence or presence of the PKTP peptide, and bound Kal-GEF1 was analyzed (Fig. 5*C*, *upper panel*). In the absence of the PKTP peptide, Kal-GEF1 did not bind to GST-SH3. However, in the presence of the PKTP peptide (~2-fold above its midpoint K_d), significant binding of GEF1 to GST-SH3 was observed. We next investigated whether the PLSP and PLPP peptides affect binding of GEF1 to Kal-SH3 (Fig. 5*C*). Again, in the presence of excess PLSP or PPLP peptide, Kal-GEF1 bound to GST-SH3. In the

and should not change upon ligand binding. Residues colored *blue* have chemical shift changes of >0.05 ppm for the PLSP peptide and >0.14 ppm for the PKTP peptide and represent site 1. Residues colored *green* have chemical shift changes of >0.14 ppm for the PKTP peptide and >0.06 ppm for the PLPP peptide and represent site 2. Changes in chemical shifts not colored in this figure are Val[21] and Ser[63] for the PLSP peptide and Glu[67] for the PKTP peptide. The canonical P*XX*P-binding site mapped in other SH3 structures is shown on the far right (colored *magenta*) *B*, alignment of Kalirin and Trio N-terminal SH3 domains from different species (*upper*) with SH3 domains of defined structure with canonical ligand-binding sites (*middle*) and non-canonical binding sites (*lower*). The frog Kalirin sequence is derived from an expressed sequence tag that is missing the N-terminal SH3 domain sequence (*dashes*). The secondary structure of Kal-SH3 is indicated above the sequences and is color-coded as described in the legend to Fig. 2. Kalirin residues that show chemical shift changes of >0.15 ppm upon binding of the PKTP peptide (330 μM) to the SH3 domain (590 μM) are colored *blue* for site 1 and *green* for site 2. Numbering is as for the structural determination of the SH3 domain. Residues colored *magenta* are ligand-binding residues observed in the structures of Fyn (Protein Data Bank code 1AON), c-Src (code 1NLP), Abl (code 1ABO), α-spectrin (α-*sp*; code 1HD3), Grb2 (N terminus; code 1AZE), c-Crk (N terminus; code 1CKA), Sem5 (C terminus; code 2SEM), GADS (code 1H3H), p67^{phox} (code 1K4U), Pex13p (code 1NM7), Grb2 (C terminus; code 1GFC), and Vav1 (code 1GCQ).

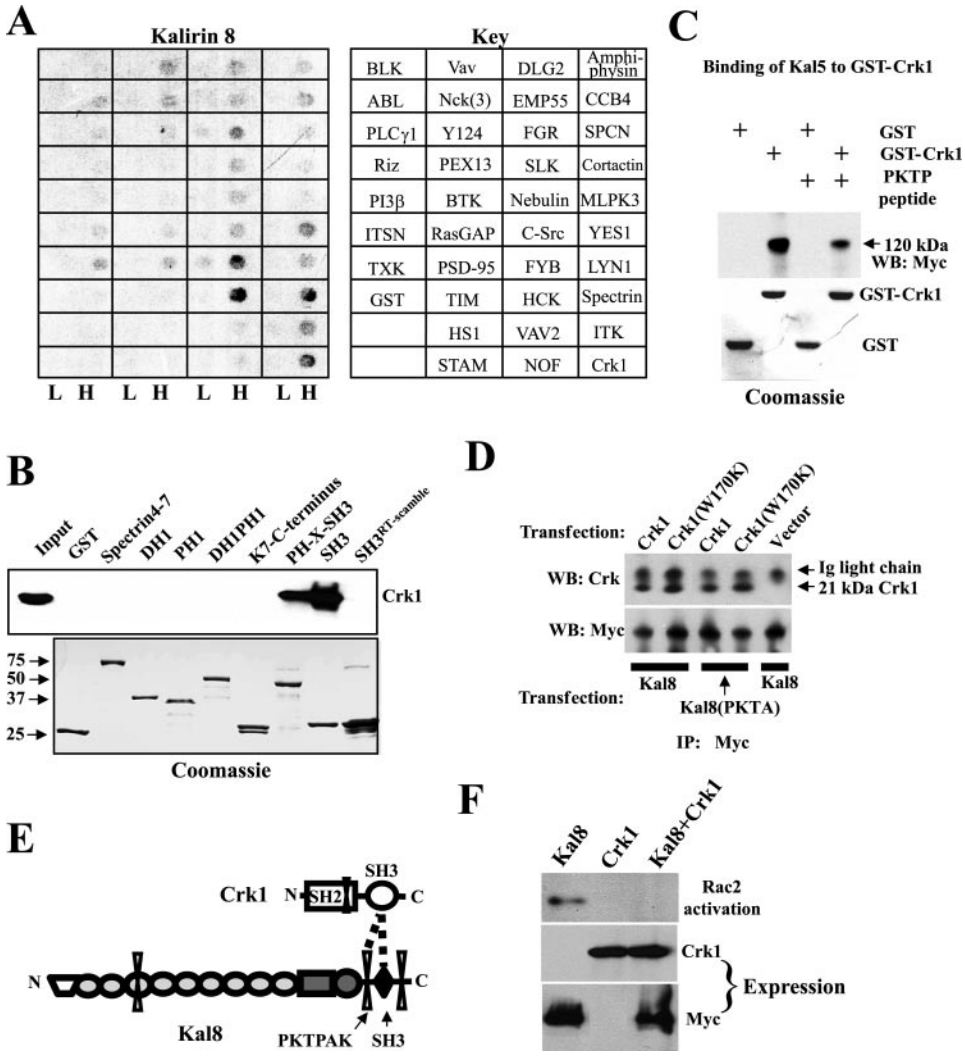

FIGURE 6. **Crk-SH3 binds to the SH3 domain and PKTPAK motif of Kalirin and inhibits its GEF activity.** *A*, shown are the results from Western analysis of Kal8 binding to SH3 domains. Cell extracts prepared from HEK-293 cells expressing Kal8 were incubated with an array containing GST or various GST-SH3 fusion proteins (80 ng (*L*) and 400 ng (*H*)). The key identifies the position of each SH3 domain protein. *PI3β*, phosphoinositide 3-kinase regulatory subunit. *B*, a GST pulldown experiment was performed to assess binding of purified Crk1 (12 ng) to different GST-Kalirin fusion proteins (2 μg). The *Input* sample represents 20% of the sample subjected to GST pulldown analysis. A Coomassie Blue-stained gel of the GST fusion proteins is shown. $SH3^{RT\text{-}scramble}$ refers to a mutant SH3 domain protein containing a scrambled RT-Src loop (^{1654}HSSE^{1657} to ^{1654}SHES^{1657}). *K7-C-terminus*, Kal7 C terminus. *C*, purified Myc-Kal5 (0.1 μg) binding to GST or GST-Crk1 (5 μg) was assessed in a GST pulldown experiment. The PKTP peptide (0.5 mM) was added as indicated. A Western blot (*WB*) with anti-Myc antibody and a Coomassie Blue-stained gel are shown. *D*, lysates prepared from 293 cells cotransfected with Myc-Kal8 or Myc-Kal8(PKTA) and with Crk1 or Crk1(W170K) were analyzed by co-immunoprecipitation. Myc-Kal8 immunoprecipitated (*IP*) with anti-Myc antibody was analyzed by Western blotting with anti-Crk and anti-Myc antibodies. *E*, a schematic representation of the regions responsible for the Kalirin/Crk interaction is shown. *F*, Crk inhibited the GEF activity of Kal8 in cells. Lysates from HEK-293 cells transfected with the vectors indicated were analyzed for Rac2 activation using the GST-Pak p21-binding domain (see "Experimental Procedures"). Cell lysates (1/25th of the pulldown sample) were analyzed for expression of transfected proteins by Western blotting with antibodies to Myc and Crk.

presence of the mutant AKTP peptide, which has vastly reduced affinity for Kal-SH3, no GEF1-SH3 domain interaction was observed, indicating that interaction of the P*XX*P peptides with the SH3 domain is required for its association with the GEF1 domain. These experiments establish a novel mechanism by which the GEF activity of Kalirin is regulated.

Crk Interacts and Co-localizes with Kalirin—Because intramolecular SH3 domain/P*XX*P interactions modestly regulate the GEF activity of Kalirin, the SH3 domain and/or adjoining PKTP ligand provides an attractive means to regulate Kalirin GEF activity by other proteins. To test this hypothesis, we sought to identify proteins that bind the PKTP sequence or the SH3 domain.

We performed a screen to identify proteins with SH3 domains that bind to Kal8. The array utilized contained 38 SH3 domains and controls. Extract from HEK-293 cells expressing exogenous Myc-Kal8 was incubated with the SH3 domain protein array, and bound Kal8 was detected by Western analysis. Kal8 bound to SH3 domains from Crk, Hck, Fyb, and α-spectrin and moderately to Fgr, Yes-1, and Itk (interleukin-2-inducible T-cell kinase); binding to control GST protein and several other SH3 domains was not observed (Fig. 6*A*). A similar profile was observed when extracts prepared from HEK-293 cells transfected with Kal5 or Kal7 (smaller Kalirin isoforms) or purified Kal5 were used, suggesting that Kalirin proteins bind directly to these SH3 domains (data not shown). Because the Crk ortholog in *C. elegans* (CED-2) genetically interacts with UNC-73 (the Kalirin paralog) in neuronal precursor cell migration and because of the established roles of Kalirin and Crk in axonal growth, we chose to focus on the interaction of Kalirin with Crk (42, 51–54).

Mapping Regions Responsible for Interaction of Kalirin with Crk1—The PKTP sequence in Kal8 is within a consensus Crk SH3 domain interaction motif (P*XX*PXK) (see Fig. 3) (55), suggesting that the linker region between the N-terminal GEF and SH3 fragment, which contains the PKTPAK sequence, is responsible for the interaction between Crk and Kalirin. To determine which regions of Kalirin interact with Crk, we examined the binding of purified recombinant chicken Crk1 to various GST-Kalirin fragments. As expected, Crk1 interacted with the PH-linker-SH3 fragment, but not with the DH1, PH1, and DH1-PH1 (GEF1) domains or with 30 amino acids of the Kal5/Kal7 C terminus (Fig. 6*B*). Quite unexpectedly, Crk1 also bound to Kal-SH3. Binding of Crk1 to Kal-SH3 was abolished in a mutant containing scrambled residues in the RT-Src loop ($SH3^{RT\text{-}scramble}$); this mutant was found not to fold by ^{15}N-edited HSQC analysis (data not shown), demonstrating an interaction of Crk1 with only the folded SH3 domain.

We next wanted to determine whether Crk1 interacts with both the PKTPAK motif and SH3 domain. Kal5, an isoform that includes the PKTPAK motif but not the SH3 domain, was purified from transfected HEK-293 cells. The purified protein was incubated with GST or GST-Crk1, and binding was assessed by Western blotting. Myc-Kal5 showed robust binding to GST-Crk1, but not to GST, demonstrating a direct

interaction (Fig. 6*C*). In the presence of excess PKTP peptide, the interaction of Kal5 with GST-Crk1 was significantly reduced, indicating that the PKTPAK motif in Kalirin binds to the SH3 domain of Crk1.

To determine whether the interaction of Crk-SH3 with the Kalirin PKTPAK motif is necessary for the interaction of Crk1 with Kalirin, we performed co-immunoprecipitation with various mutant Kal8 and Crk1 proteins. Lysates were prepared from HEK-293 cells transfected with wild-type Kal8, wild-type Crk1, or Crk1(W170K), which harbors a mutation that blocks the interaction of its SH3 domain with its P*XX*P ligands (43). Both wild-type Crk1 and Crk1(W170K) co-immunoprecipitated with Myc-Kal8 (Fig. 6*D*). Wild-type and mutant Crk1 also co-immunoprecipitated with Kal8 containing a mutation in its consensus Crk-binding motif (Kal8(PKTA)), but not from control cells transfected with empty vector. Crk also co-immunoprecipitated with Kalirin from embryonic day 17 mouse brain (data not shown). These experiments indicate the Kalirin PKTPAK motif is not necessary for the interaction of Kalirin with Crk1, whereas Kal-SH3 is necessary for this interaction (Fig. 6*D*).

We next mapped the region of Crk1 bound to Kalirin. Crk1 contains single SH2 and SH3 domains (Fig. 6*E*). Chicken Crk1 contains a P*XX*P ligand within its SH2 domain (NP_001007847), which could serve as a ligand for Kal-SH3. However, purified Kal8 binding to GST-Crk1-SH2 was similar to background binding observed with GST, indicating that neither Crk1-SH2 nor its P*XX*P motifs are involved in binding Kalirin (data not shown).

GST-Crk1-SH3 interacted with Kal8 in the SH3 array experiment (Fig. 6*A*), and the SH3 domain of Kalirin was necessary for this interaction. These results unexpectedly indicate that Kal-SH3 binds to Crk1-SH3. Together, the results of these mapping experiments indicate that Crk1-SH3 forms a bidentate interaction with both the Kalirin PKTPAK motif and Kal-SH3 (Fig. 6*E*).

Crk Negatively Regulates the GEF Activity of Kalirin—Because the SH3 domain/PKTP region of Kalirin regulates its GEF activity and because Crk binds this region, we suspected that Crk would affect Kalirin GEF activity. To test this hypothesis, the levels of activated Rac in cells were measured using an effector-based assay (41, 45, 56). Reverse transcription-PCR analysis of HEK-293 cells identified Rac2, not Rac1 or Rac3; human Rac1 has 92% amino acid identity to Rac2. Kinetic analysis of Kal-GEF1 in fluorogenic exchange assays showed that, like Rac1, Rac2 is a good substrate ($k_{cat} = 30 \pm 0.4\ h^{-1}$ and $K_m = 2.6 \pm 0.5\ \mu M$) (41) (data not shown). Therefore, the p21-binding domain of Pak was used to compare the levels of activated Rac2 in HEK-293 cells expressing Kal8, Crk1, or both proteins (Fig. 6*F*). Expression of Kal8 produced significant activation of Rac2, whereas expression of Crk1 did not (Fig. 6*F*). Coexpression of Crk1 completely eliminated the ability of Kal8 to activate Rac2 (Fig. 6*F*). The activity assays, together with the GST binding and co-immunoprecipitation experiments, showed that the interaction of Crk with Kalirin nearly completely eliminated GEF activity. Therefore, the intermolecular interaction of Crk1 with the Kal-SH3/linker region potently inhibits its GEF activity; in contrast, intramolecular interactions in this region of Kalirin may be more important for fine-tuning GEF activity.

DISCUSSION

Structure of Kal-SH3—The three-dimensional fold of Kal-SH3 is similar to that of other SH3 domains, as exemplified by comparison with the Sem5 SH3 domain structure (Fig. 2*E*). The major differences in the backbone overlay are in the n-Src and distal Src loops, which are longer in Kalirin. The divergence of the Kalirin n-Src loop from the structures of other SH3 domains is interesting because residues in this loop are involved in a novel P*XX*P ligand-binding site(s). Although a *cis*-Pro in the distal loop does not directly contribute to this binding site(s), it provides a potentially attractive means of regulating ligand binding through *cis,trans*-isomerization. Similarly, in the RhoGEF protein Vav, an Ile–*cis*-Pro bond in its N-terminal SH3 domain positions the RT-Src loop in an orientation that blocks the canonical P*XX*P-binding site, whereas the *trans*-Pro form does not (38).

Cooperative Binding of PXXP Ligands to Novel Site(s) on Kal-SH3—We originally hypothesized that Kal-SH3 would bind through either an intra- or intermolecular interaction with P*XX*P ligands at the canonical P*XX*P-binding site observed in many other SH3 structures. We were surprised that the three different internal P*XX*P motifs tested interacted instead with a novel site(s), with the PKTP ligand showing cooperative binding.

Lack of binding to the canonical SH3 domain ligand-binding site may be due to the limited number of P*XX*P peptides tested and failure to identify the correct *in vivo* ligand; however, we favor the hypothesis that Kal-SH3 has unique site(s) for binding P*XX*P peptides. Several hydrophobic residues that form the hydrophobic pockets in other SH3 domains that accommodate the Pro residues in the P*XX*P polyproline type II helix are not conserved in Kalirin (Fig. 4*B*) (57). Based on known SH3 domain structures, Gln^{24} in Kalirin should be Phe or Trp; in addition, several hydrophobic residues expected in the 3_{10} helix are absent from Kalirin.

Trp^{54} is a canonical P*XX*P ligand-binding residue that is conserved in nearly all SH3 domains; mutation of this residue generally blocks ligand interaction (14, 58, 59). Consistent with our identification of a different binding site(s), the corresponding Trp residue is not conserved in all Kalirin homologs. Mutation of this conserved Trp residue in the Trio N-terminal SH3 domain disrupts neurite outgrowth (14); however, based on our analysis of a Kal-SH3 mutant containing a scrambled RT-Src loop, this mutation may disrupt folding of the SH3 domain. Searching >2400 SH3 domain sequences in the SMART Database has revealed several other SH3 domains that lack this Trp residue (A57152, XP_044334, KIAA0318, NP_058589, Q62270, NP_498918, NP_004758, and NP_508660), suggesting that these SH3 domains interact with proline-rich ligands at an alternative site, as Kalirin does. Consistent with this hypothesis, mutation of the corresponding Trp residue in PSD-95 does not block an intramolecular SH3 domain/ligand interaction (16).

Titration of Kal-SH3 with the PKTP peptide yielded a cooperative binding isotherm for all residues showing chemical shift changes and a Hill coefficient of >2, suggesting multiple binding sites for the PKTP ligand. Few cooperative binding isotherms have been observed in chemical shift titration experiments. Analysis of the P*XX*P ligand binding to the Sem5 SH3 domain showed that residues in the RT-Src loop do not contact ligand, but have significant cooperative changes in chemical shifts (60). Similar large changes in chemical shifts of residues in the RT-Src loop of Kal-SH3 are observed upon binding of P*XX*P peptides. Because the PLSP peptide (which does not bind to the RT-Src loop) also produces these changes in chemical shifts, this may be an intrinsic cooperative communication between sites 1 and 2 in Kal-SH3. Cooperative binding of three calcium ions to yeast calmodulin has been observed in chemical shift titration experiments (61). This cooperativity derives from an interaction of the N- and C-terminal calcium-binding domains of calmodulin that affects their affinity for calcium. In our study, cooperativity suggests that a single SH3 domain contains two P*XX*P-binding sites.

Surface mapping of Kal-SH3 residues with ligand-induced chemical shift changes provided support for the two-site model. The PKTP peptide bound to clusters of residues in sites 1 and 2, whereas the PLSP

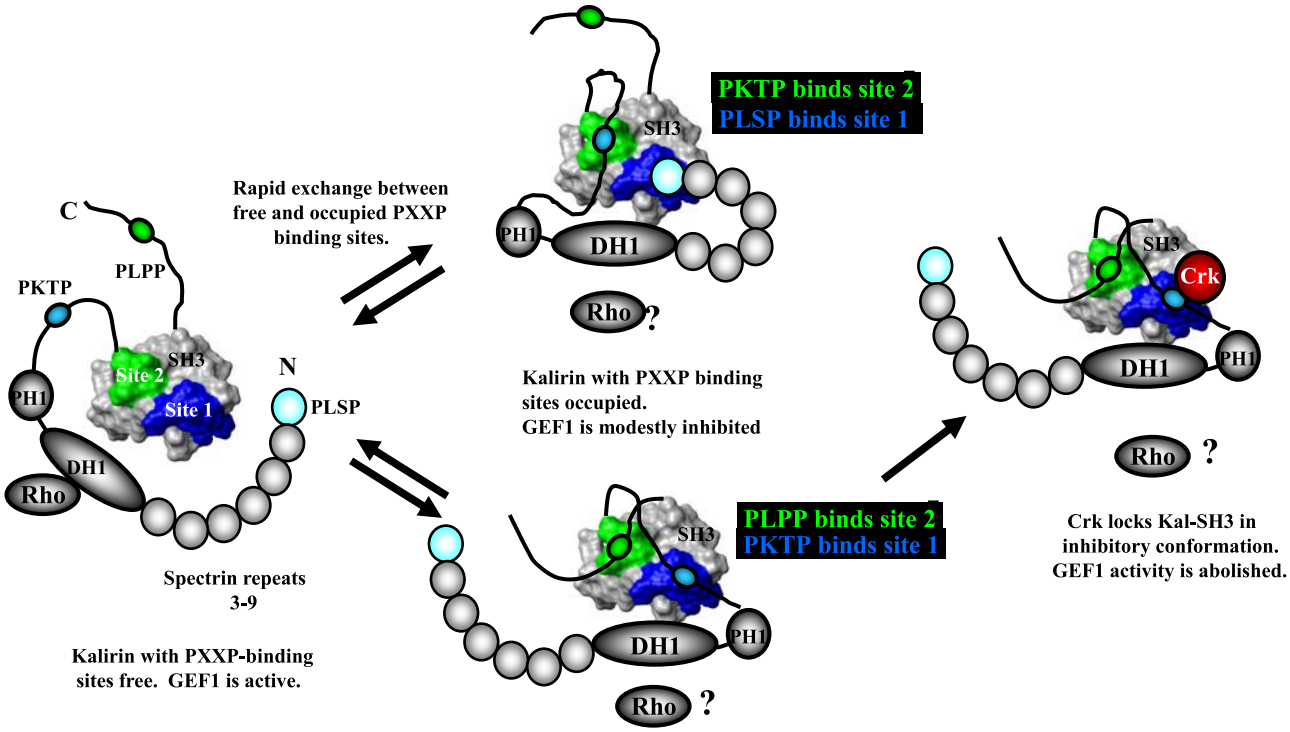

FIGURE 7. **Model of how intramolecular SH3 domain/ligand interactions and intermolecular Kalirin/Crk binding affect GEF activity.** Although our data strongly support two P*XX*P-binding sites in Kal-SH3, as depicted in this model (with site 1 colored *blue* and site 2 colored *green*), we cannot rule out a single P*XX*P-binding site. The PKTP ligand is indicated by *light blue ovals*, and the PLPP ligand by *green ovals*. Crk is colored *red*. The PLSP ligand is located in spectrin repeat 3 (colored *cyan*). The Sec14p domain and two N-terminal spectrin repeats in Kal8 are not shown.

peptide in spectrin repeat 3 affected residues only in site 1. Site 1 involves several residues from the RT-Src and n-Src loops; the n-Src loop is longer in Kalirin and Trio than in many other SH3 domains. The PLPP peptide bound primarily to site 2. Site 2 involves segments of the β1, β4, and β6 sheets. Although the chemical shift titration experiments identified two clusters of residues located immediately proximal to each other, additional residues were affected. Although we cannot rule out the possibility that there is a single P*XX*P-binding site, the cooperative binding isotherms, Hill plots, chemical shift mapping, and evolutionary conservation of P*XX*P-binding sites strongly support a two-site model.

It is clear that the P*XX*P peptides tested did not interact with Kal-SH3 at a canonical P*XX*P-binding site. Non-canonical SH3 domain ligand-binding sites have been described in Grb2, Pex13p, Vav, and p67^{phox} (Fig. 4*B*, *lower*) (59, 62–64). Furthermore, the OB-fold is very similar to the SH3 domain fold and binds oligonucleotides or oligosaccharides (65). Additional studies will be required to determine whether Kal-SH3 contains one or two P*XX*P-binding sites and whether the P*XX*P ligands bind Kal-SH3 by adopting a polyproline type II helix structure. The AKTP and tPKTA peptides, which each lack one key Pro residue, bind with 30-fold lower affinity, indicating that both prolines are important for binding.

It is possible that peptide binding to Kal-SH3 does not mimic an intermolecular interaction in full-length Kalirin. However, we have compared ^{15}N-edited HSQC spectra of Kal-SH3 and Kal-SH3 with saturating PKTP peptide with a spectrum of the PH-linker-SH3 domain fragment (data not shown). This spectrum shows resonances that are consistent with the PKTP sequence being bound to the SH3 domain. Therefore, this experiment supported the presence of an intramolecular SH3 domain/PKTP interaction in full-length Kalirin.

The SH3 Domain of Kalirin Inhibits Its GEF Activity through an Intramolecular Interaction—Kal-SH3 bound to Kal-GEF1 and inhibited its GEF activity only when in the presence of a P*XX*P peptide (Fig. 5, *A* and *C*), suggesting that the SH3 domain/peptide interaction mediates binding to Kal-GEF1. All three P*XX*P motifs in Kal8 can bind to Kal-SH3 individually or in two possible configurations (based on surface mapping experiments; see model in Fig. 7). Although mutation of any individual P*XX*P motif did not affect the GEF activity of Kal8, mutation of all three P*XX*P motifs (Kal8ΔP*XX*P) resulted in a modest 1.5-fold increase in GEF activity. When a single P*XX*P is mutated, one or two of the remaining P*XX*P motifs can presumably bind Kal-SH3 and inhibit its GEF activity. In summary, we think that Kal8ΔP*XX*P has more activity that Kal8 because it does not allow binding of the SH3 domain to any of the P*XX*P ligands and thus blocks interaction of the SH3 domain-P*XX*P complex with the proximal GEF1 domain. Binding of the SH3 domain-P*XX*P complex to GEF1 may sterically reduce the accessibility of Kal-GEF1 to its substrate.

The relatively weak intramolecular SH3 domain/P*XX*P interactions provide an attractive mode of modulation. Disruption of intramolecular SH3 domain/P*XX*P interactions would enhance GEF activity and generate two new binding sites (Kal-SH3 and P*XX*P) for intermolecular interactions. This mode of regulation is known for Itk, a kinase that is activated when Grb2 or Sam68 binds to both its SH3 domain and P*XX*P motif (17). In support of our findings of SH3 domain regulation of Rho-GEFs, an intramolecular SH3 domain-mediated regulation of Ost was suggested previously based on the transformation activity of several splice variants of rat Ost (human ortholog called Dbs) (13).

Several mechanisms may be needed to fine-tune levels of GEF activity and to control their potent effects on cells. Like Kalirin, many RhoGEFs have SH3 domains preceding or following their GEF domains (Fig. 1). Eight of these 22 human RhoGEFs also contain putative intramolecular P*XX*P ligands between their GEF and SH3 domains. Because some SH3 domains recognize non-canonical ligands, intramolecular SH3 domain-ligand complexes may be relevant to the regulation of other RhoGEFs as well (59, 63, 64, 66). For example, one of the five SH3 domains in inter-

sectin associates with a non-canonical SH3 domain ligand in its Dbl homology domain, resulting in inhibition of Cdc42 binding and GEF activity toward this Rho GTPase (67). Although its effects on GEF activity have not been investigated, binding of a P*XX*P motif in the faciogenital dysplasia RhoGEF Fgd1 to the cortactin SH3 domain plays a role in actin assembly (68).

Crk Is a Kalirin-binding Partner That Inhibits GEF Activity—To identify SH3 domain ligands that might disrupt intramolecular Kal-SH3/P*XX*P interactions, we used an SH3 domain array. The screen identified Crk, which also co-immunoprecipitated and co-localized with Kalirin. This interaction is consistent with the fact that the N-terminal SH3 domains of Crk and cortactin are the only SH3 domains known to prefer the binding motif P*XX*PXK, which is present in Kalirin (55, 69). Furthermore, the connection between Crk and Kalirin is supported by the observation that the Crk ortholog in *C. elegans* (CED-2) genetically interacts with the Kalirin ortholog (UNC-73) in P-cell migration (51). Src, Yes, spectrin, Fyb, and Fgr were also identified in the SH3 domain screen and may also have functions associated with Kalirin.

GST pulldown and co-immunoprecipitation experiments demonstrated an interaction of Crk1-SH3 with both the P*XX*PXK motif and Kal-SH3. Although the observation of Crk1/Kalirin SH3 domain heterodimers was surprising, the structures of other SH3 domains have revealed direct dimeric SH3/SH3 domain contacts (29, 70). Like the intramolecular Kalirin SH3 domain-PKTP motif complex, the intermolecular Kal8-Crk complex strongly inhibited GEF activity toward Rac. Likely explanations for the observed inhibition are that Crk locks the intramolecular Kal-SH3 P*XX*P ligand into an inhibitory conformation, disrupting an internal SH3 domain/P*XX*P interaction, allosterically affecting Kalirin GEF activity, or sterically hindering the association of GEF with Rac (Fig. 7). We do not know what factors or cellular events relieve Crk-mediated inhibition of Kal8. One intriguing possibility is that stimulation of TrkA, a neurotrophin receptor, with nerve growth factor liberates Crk-mediated inhibition of Kalirin. This hypothesis is supported by the interaction of the Kalirin N-terminal PH domain (part of the GEF1 domain) with TrkA, enhancement of nerve growth factor-induced activation of Rac by Kalirin expression, and the important role of Crk in pathways downstream of TrkA (52, 54, 71, 72). Further experimentation will be required to decipher the complexities of the SH3 domain/ligand interactions that control Kalirin GEF activity.

Acknowledgments—We greatly appreciate the support of Dr. Richard Mains. We thank Dr. Bruce Mayer for helpful discussions and providing the Crk1, Crk2, and Crk1(W170K) expression constructs and purified GST-Crk fusion proteins. We appreciate the effort of Kevin McFadgen in processing NMR chemical shift titration data. We appreciate the laboratory assistance of Yanping Wang and thank Dr. Henry Keutmann for synthesis of the many peptides used in this study.

REFERENCES

1. Rossman, K. L., Der, C. J., and Sondek, J. (2005) *Nat. Rev. Mol. Cell Biol.* **6,** 167–180
2. Zheng, Y. (2002) *Trends Biochem. Sci.* **25,** 724–732
3. Kutsche, K., Yntema, H., Brandt, A., Jantke, I., Nothwang, H. G., Orth, U., Boavida, M. G., David, D., Chelly, J., Fryns, J. P., Moraine, C., Ropers, H. H., Hamel, B. C. J., van Bokhoven, H., and Gal, A. (2000) *Nat. Genet.* **26,** 247–250
4. Aghazadeh, B., Lowry, W. E., Huang, X. Y., and Rosen, M. K. (2000) *Cell* **102,** 625–633
5. Das, B., Shu, X., Day, G. J., Han, J., Krishna, U. M., Falck, J. R., and Broek, D. (2000) *J. Biol. Chem.* **275,** 15074–15081
6. Russo, C., Gao, Y., Mancini, P., Vanni, C., Porotto, M., Falasca, M., Torrisi, M. R., Zheng, Y., and Eva, A. (2001) *J. Biol. Chem.* **276,** 19524–19531
7. Bi, F., Debreceni, B., Zhu, K., Salani, B., Eva, A., and Zheng, Y. (2001) *Mol. Cell. Biol.* **21,** 1463–1474
8. Kubiseski, T. J., Culotti, J., and Pawson, T. (2003) *Mol. Cell. Biol.* **23,** 6823–6835
9. Han, J., Luby-Phelps, K., Das, B., Shu, X., Xia, Y., Mosteller, R. D., Krishna, U. M., Falck, J. R., White, M. A., and Broek, D. (1998) *Science* **279,** 558–560
10. Crompton, A. M., Foley, L. H., Wood, A., Roscoe, W., Stokoe, D., McCormick, F., Symons, M., and Bollag, G. (2000) *J. Biol. Chem.* **275,** 25751–25759
11. Fleming, I. N., Gray, A., and Downes, C. P. (2000) *Biochem. J.* **351,** 173–182
12. Yoshii, S., Tanaka, M., Otsuki, Y., Wang, D. Y., Guo, R. J., Zhu, Y., Takeda, R., Hanai, H., Kaneko, E., and Sugimura, H. (1999) *Oncogene* **18,** 5680–5690
13. Lorenzi, M. V., Castagnino, P., Chen, Q., Hori, Y., and Miki, T. (1999) *Oncogene* **18,** 4742–4755
14. Estrach, S., Schmidt, S., Diriong, S., Penna, A., Blangy, A., Fort, P., and Debant, A. (2002) *Curr. Biol.* **12,** 307–312
15. Kay, B. K., Williamson, M. P., and Sudol, P. (2000) *FASEB J.* **14,** 231–241
16. Mayer, B. J. (2001) *J. Cell Sci.* **114,** 1253–1263
17. Andreotti, A. H., Bunnell, S. C., Feng, S., Berg, L. J., and Schreiber, S. L. (1997) *Nature* **385,** 93–97
18. Hansson, H., Okoh, M. P., Smith, C. I., Vihinen, M., and Hard, T. (2001) *FEBS Lett.* **489,** 67–70
19. Moarefi, I., LaFevre-Bernt, M., Sicheri, F., Huse, M., Lee, C. H., Kuriyan, J., and Miller, W. T. (1997) *Nature* **385,** 650–653
20. Lerner, E. C., and Smithgall, T. E. (2002) *Nat. Struct. Biol.* **9,** 365–369
21. Barila, D., and Superti-Furga, G. (1998) *Nat. Genet.* **18,** 280–282
22. Brazin, K. N., Futton, D. B., and Andreotti, A. H. (2000) *J. Mol. Biol.* **302,** 607–623
23. Pursglove, S. E., Mulhern, T. D., Mackay, J. P., Hinds, M. G., and Booker, G. W. (2002) *J. Biol. Chem.* **277,** 755–762
24. Pluk, H., Dorey, K., and Superti-Furga, G. (2002) *Cell* **108,** 247–259
25. Brasher, B. B., Roumiantsev, S., and Van Etten, R. A. (2001) *Oncogene* **20,** 7744–7752
26. Zhang, H., and Gallo, K. A. (2001) *J. Biol. Chem.* **276,** 45598–45603
27. Ago, T., Kuribayashi, F., Hiroaki, H., Takeya, R., Ito, T., Kohda, D., and Sumimoto, H. (2003) *Proc. Natl. Acad. Sci. U. S. A.* **100,** 4474–4479
28. Groemping, Y., Lapouge, K., Smerdon, S. J., and Rittinger, K. (2003) *Cell* **113,** 343–355
29. Yuzawa, S., Ogura, K., Horiuchi, M., Suzuki, N. N., Fujioka, Y., Kataoka, M., Sumimoto, H., and Inagaki, F. (2004) *J. Biol. Chem.* **279,** 29752–29760
30. Tavares, G. A., Panepucci, E. H., and Brunger, A. T. (2001) *Mol. Cell* **8,** 1313–1325
31. Seabold, G. K., Burette, A., Lim, I. A., Weinberg, R. J., and Hell, J. W. (2003) *J. Biol. Chem.* **278,** 15040–15048
32. Delaglio, F., Grzesiek, S., Vuister, G. W., Zhu, G., Pfeifer, J., and Bax, A. (1995) *J. Biomol. NMR* **6,** 277–293
33. Bartels, C., Xia, T., Billeter, M., Guntert, P., and Wuthrich, K. (1995) *J. Biomol. NMR* **6,** 1–10
34. Guntert, P., Mumenthaler, C., and Wuthrich, K. (1997) *J. Mol. Biol.* **273,** 283–298
35. Vuister, G. W., Delaglio, F., and Bax, A. (1993) *J. Biomol. NMR* **3,** 67–80
36. Vuister, G. W., and Bax, A. (1993) *J. Am. Chem. Soc.* **115,** 7772–7777
37. Cornilescu, G., Delaglio, F., and Bax, A. (1999) *J. Biomol. NMR* **13,** 289–302
38. Ogura, K., Nagata, K., Horiuchi, M., Ebisui, E., Hasuda, T., Yuzawa, S., Nishida, M., Hatanaka, H., and Inagaki, F. (2002) *J. Biomol. NMR* **22,** 37–46
39. Zhang, B., Zhang, Y., Wang, Z., and Zheng, Y. (2000) *J. Biol. Chem.* **275,** 25299–25307
40. Snyder, J. T., Worthylake, D. K., Rossman, K. L., Betts, L., Pruitt, W. M., Siderovski, D. P., Der, C. J., and Sondek, J. (2002) *Nat. Struct. Biol.* **9,** 468–475
41. Schiller, M. R., Blangy, A., Huang, J. P., Mains, R. E., and Eipper, B. A. (2005) *Exp. Cell Res.* **307,** 402–417
42. May, V., Schiller, M. R., Eipper, B. A., and Mains, R. E. (2002) *J. Neurosci.* **22,** 6980–6990
43. Tanaka, M., Gupta, R., and Mayer, B. J. (1995) *Mol. Cell. Biol.* **15,** 6829–6837
44. Husten, E. J., and Eipper, B. A. (1994) *Arch. Biochem. Biophys.* **312,** 487–492
45. Penzes, P., Johnson, R. C., Alam, M. R., Kambampati, V., Mains, R. E., and Eipper, B. A. (2000) *J. Biol. Chem.* **275,** 6395–6403
46. Brunger, A. T. (1992) *X-PLOR (Version 3.1): A System for X-ray Crystallography and NMR*, Yale University Press, New Haven, CT
47. Holm, L. F., and Sander, C. (1993) *J. Mol. Biol.* **233,** 123–138
48. Bolam, D. N., Ciruela, A., McQueen-Mason, S., Simpson, P., Williamson, M. P., Rixon, J. E., Boraston, A., Hazlewood, G. P., and Gilbert, H. J. (1998) *Biochem. J.* **331,** 775–781
49. Gmeiner, W. H., Xu, I., Horita, D. A., Smithgall, T. E., Engen, J. R., Smith, D. L., and Byrd, R. A. (2001) *Cell Biochem. Biophys.* **35,** 115–126
50. Vaynberg, J., Fukuda, T., Chen, K., Vinogradova, O., Velyvis, A., Tu, Y., Ng, L., Wu, C., and Qin, J. (2005) *Mol. Cell* **17,** 513–523
51. Spencer, A. G., Orita, S., Malone, C. J., and Han, M. (2001) *Proc. Natl. Acad. Sci. U. S. A.* **98,** 13132–13137
52. Teng, K. K., Lander, H., Fajardo, J. E., Hanafusa, H., Hempstead, B. L., and Birge, R. B. (1995) *J. Biol. Chem.* **270,** 20677–20685
53. Feller, S. M. (2001) *Oncogene* **20,** 6348–6371
54. Weinstein, D. E., Dobrenis, K., and Birge, R. B. (1999) *Dev. Brain Res.* **116,** 29–39
55. Wu, X., Knudsen, B., Feller, S. M., Zheng, J., Sali, A., Cowburn, D., Hanafusa, H., and Kuriyan, J. (1995) *Structure* (*Lond.*) **3,** 215–226

56. Bagrodia, S., Taylor, S. J., Creasy, C. L., Chernoff, J., and Cerione, R. A. (1995) *J. Biol. Chem.* **270,** 22731–22737
57. Larson, S. M., and Davidson, A. R. (2000) *Protein Sci.* **9,** 2170–2180
58. Hing, H., Xiao, J., Harden, N., Lim, L., and Zipursky, S. L. (1999) *Cell* **97,** 853–863
59. Nishida, M., Nagata, K., Hachimori, Y., Horiuchi, M., Ogura, K., Mandiyan, V., Schlessinger, J., and Inagaki, F. (2001) *EMBO J.* **20,** 2995–3007
60. Ferreon, J. C., and Hilser, V. J. (2003) *Protein Sci.* **12,** 982–996
61. Nakashima, K., Ishida, H., Ohki, S., Hikichi, K., and Yazawa, M. (1999) *Biochemistry* **38,** 98–104
62. Barnett, P., Bottger, G., Klein, A. T., Tabak, H. F., and Distel, B. (2000) *EMBO J.* **19,** 6382–6391
63. Pires, J. R., Hong, X., Brockmann, C., Volkmer-Engert, R., Schneider-Mergener, J., Oschkinat, H., and Erdmann, R. (2003) *J. Mol. Biol.* **326,** 1427–1435
64. Kami, K., Takeya, R., Sumimoto, H., and Kohda, D. (2002) *EMBO J.* **21,** 4268–4276
65. Murzin, A. G. (1993) *EMBO J.* **12,** 861–867
66. Harkiolaki, M., Lewitzky, M., Gilbert, R. J., Jones, E. Y., Bourette, R. P., Mouchiroud, G., Sondermann, H., Moarefi, I., and Feller, S. M. (2003) *EMBO J.* **22,** 2571–2582
67. Zamanian, J. L., and Kelly, R. B. (2003) *Mol. Biol. Cell* **14,** 1624–1637
68. Kim, K., Hou, P., Gorski, J. L., and Cooper, J. A. (2004) *Biochemistry* **43,** 2422–2427
69. Sparks, A. B., Rider, J. E., Hoffman, N. G., Fowlkes, D. M., Quillam, L. A., and Kay, B. K. (1996) *Proc. Natl. Acad. Sci. U. S. A.* **93,** 1540–1544
70. Kishan, K. V., Scita, G., Wong, W. T., Di Fiore, P. P., and Newcomer, M. E. (1997) *Nat. Struct. Biol.* **4,** 739–743
71. Chakrabarti, K., Lin, R., Schiller, N. I., Wang, Y., Fan, Y.-X., Koubi, D., Rudkin, B. B., Johnson, G. R., and Schiller, M. R. (2005) *Mol. Cell. Biol.* **25,** 5106–5118
72. York, R. D., Yao, H., Dillon, T., Ellig, C. L., Eckert, S. P., McCleskey, E. W., and Stork, P. J. (1998) *Nature* **392,** 622–626

Regulation of RhoGEF Activity by Intramolecular and Intermolecular SH3 Domain Interactions

Martin R. Schiller, Kausik Chakrabarti, Glenn F. King, Noraisha I. Schiller, Betty A. Eipper and Mark W. Maciejewski

J. Biol. Chem. 2006, 281:18774-18786.
doi: 10.1074/jbc.M512482200 originally published online April 27, 2006
